Simplified two-dimensional numerical modelling of coastal flooding and example applications

Paul D. Bates[a,1], Richard J. Dawson[b], Jim W. Hall[b], Matthew S. Horritt[a], Robert J. Nicholls[c], Jon Wicks[d] and Mohamed Ahmed Ali Mohamed Hassan[e]

a. *School of Geographical Sciences, University of Bristol, University Road, Bristol, BS8 1SS, UK*

b. *School of Civil Engineering and Geosciences, University of Newcastle upon Tyne, Cassie Building, Newcastle upon Tyne, NE1 7RU, UK*

c. *School of Civil Engineering and the Environment and Tyndall Centre for Climate Change Research, Southampton University, Southampton. S017 1BJ, UK*

d. *Halcrow Ltd., Burderup Park, Swindon, Wiltshire, SN4 0QD, UK*

e. *HR Wallingford Ltd, Wallingford, UK*

Submitted to *Coastal Engineering*

Last saved at: 16/05/2005 3:17 PM

Number of words: 10001

[1] Contact Author. *Tel*: +44-117-928-9108. *Fax*: +44-117-928-9108. *E-mail*: Paul.Bates@Bristol.ac.uk

Abstract

In this paper we outline the development and application of a simple two-dimensional hydraulic model for use in assessments of coastal flood risk. Such probabilistic assessments typically need evaluation of many thousands of model simulations and hence computationally efficient codes of the type described here are required. The code, LISFLOOD-FP, uses a storage cell approach discretized as a regular grid and calculates the flux between cells explicitly using analytical relationships derived from uniform flow theory. The resulting saving in computational cost allows fine spatial resolution simulations of regional scale flooding problems within minutes or a few hours on a standard desktop PC. The development of the code for coastal applications is described, followed by an evaluation of its performance against four test cases representing a variety of flooding problems at different scales. For three of these cases an observed flood extent is available to compare to model predictions. In each case the model is able to match the observed shoreline to within the error of the of the observed flow, topography and validation data and outperforms a non-model flood extent prediction made using a simple Geographical Information System (GIS) technique.

Key words

Coastal flooding, 2D numerical modelling, inundation, defence overtopping, sea level rise

1. Flood risk assessment for coastal planning

Evaluation of coastal flood risk is a key requirement in hazard management and planning at national, regional and local scales given the significant proportion of the world's population that reside in the coastal zone. In 1990 this amounted to 1.2 billion people in the area within 100km distance and 100m elevation of the coastline, at densities about three times the global mean (Small and Nicholls, 2003). The area also includes a high concentration of the world's biggest cities (Nicholls, 1995) and produces a considerable portion of global GDP (Turner *et al*., 1996). Coastal development is already threatened by a range of natural hazards such as storm surges, storm waves and tsunamis. Moreover human–induced changes such as dredging, land reclamation and coastal defence are impacting on the natural behaviour of the coastal zone and changing the risk of flooding and storm damage. Climate change, in particular sea level rise (SLR), is an additional pressure that could greatly increase the risk of flooding in the coastal zone (Nicholls, 2002). Therefore, strategic assessment of coastal flooding and its implications needs to be conducted within a risk-based framework that is capable of evaluating both current and possible future conditions.

Considerable progress has been made in recent years in the development of methodologies for risk assessment and risk-based management of the coast (Vrijling, 1993; Meadowcroft *et al.,* 1996; USACE, 1996; Reeve, 1998; Voortman, 2002; Hall *et al*., 2003). Risk assessment provides a rational basis for the development of coastal flood management policy, allocation of resources and for monitoring the performance of coastal management activities at local, regional and national scales in a transparent and auditable manner. At the heart of all methods to assess coastal flood risk is a requirement to predict water levels and inundation extent that will result from particular combinations of process drivers such as meteorological conditions, tidal conditions, defence systems and their associated likelihood of failure

(Dawson *et al.*, 2003; Dawson *et al.*, 2005). Such predictions are typically obtained from numerical hydrodynamic models. For coastal flows two-dimensional horizontal solutions of the Shallow Water equations are considered to be the current state-of-the-art (Madsen and Jacobsen, 2004, p282). In shallow coastal seas and well mixed estuaries such models can provide a realistic simulation of water levels (Battjes and Gerritsen, 2002; Sutherland *et al.*, 2004) and have good forecasting capabilities (Madsen and Jacobsen, 2004). In application, such models require accurate topographic and bathymetric data at a scale commensurate with the flow features that the user wishes to resolve. For accurate damage appraisal of flooding in urban areas located in the coastal zone this may require model grid scales of 50m or less. Hence, while such models can be applied at scales appropriate to shoreline management plans (50-200km), full two-dimensional solutions incur a significant computational cost, particularly when applied at regional scales.

Risk-based assessments require the evaluation of many different combinations of meteorological, tidal and defence conditions within a probabilistic framework (see Dawson *et al.*, 2005). For any realistic coastal defence system, this may require the analysis of thousands of inundation simulations, even if the model output is treated as deterministic. Moreover, recent research has shown that the assumption of a deterministic inundation model may be highly questionable (Aronica *et al*., 2002). In reality, many combinations of model structures, data and parameters may fit sparse calibration and validation data equally well, yet these realisations may give very different spatial predictions of water level over the whole domain. The need to evaluate the behaviour of multiple parameter sets, all of which may be equally likely, will compound significantly the computational demands of a risk assessment. Under different forcing conditions the differences between parameter sets that fit the calibration event data equally well may be even more pronounced (see Beven, 2002 for a discussion of uncertainty in environmental modelling). Over the last 13 years, much work

has focussed on the characterization of uncertainty in numerical model output (see Beven and Binley, 1992; Beven *et al.*, 2000; Beven and Freer, 2001) and this has also been extended to the consideration of uncertainty in fluvial flood inundation prediction (Romanowicz *et al.,* 1996; Aronica *et al.*, 1998; Romanowicz and Beven, 1998; Aronica *et al.* 2002; Romanowicz and Beven, 2003; Bates *et al.*, 2004). Similar to flood risk assessment, such uncertainty analysis is normally performed using Monte Carlo analysis and may require evaluation of many thousands of model realisations.

A considerable need therefore exists to develop simplified two-dimensional models for coastal flooding that can be used within a risk-based framework. Such models should be capable of capturing the dominant physical mechanisms of coastal flood hydrodynamics, but at a substantially reduced computational cost. Simplified two-dimensional approaches have been developed over the last decade for fluvial flooding problems (see Estrela and Quintas, 1994; Bechteler *et al.*, 1994; Romanowicz *et al.* 1996; Bates and De Roo, 2000; Dhondia and Stelling, 2002; Venere and Clausse, 2002) to take advantage of the increased availability of high accuracy, fine spatial resolution topographic data now available from remote sensing methodologies such as airborne laser altimetry (Gomes-Pereira and Wicherson, 1999). For fluvial flooding such models have been shown (e.g., Horritt and Bates, 2002) to perform as well as full two-dimensional models at predicting maximum inundation during dynamic events. This is based on validation against observed inundation extent data obtained from airborne photography and satellite Synthetic Aperture Radars. However, such techniques have yet to be comprehensively applied or tested for coastal flooding. In theory, such methods should work equally well in such zones and be capable of wide area application at fine (250m or less) spatial resolution. However, we need to determine the extent to which simplification of the physical mechanisms represented in the model compromises the accuracy of the results obtained given data and calibration uncertainties.

The purpose of this paper is therefore twofold:

1. to outline a simplified two-dimensional fluvial hydraulic model, LISFLOOD-FP, and describe its development for application in the coastal zone,

2. to evaluate the model performance for a variety of coastal test cases, and where possible compare model predicted inundation extent to observed data.

2. The LISFLOOD-FP model

The LISFLOOD-FP code originally developed by Bates and De Roo (2000) was chosen as the basis for all simulations reported in this paper. This code has been shown to be computationally efficient (e.g. Aronica *et al.*, 2002) and to yield good predictions of maximum inundation extent for fluvial flooding problems (e.g. Bates and De Roo, 2000; Horritt and Bates, 2001a and b; Horritt and Bates, 2002). LISFLOOD-FP is a coupled 1D/2D hydraulic model based on a raster grid. Effectively, flooding is treated using an intelligent volume-filling process based on hydraulic principles and embodying the key physical notions of mass conservation and hydraulic connectivity. Channel flow is handled using a one-dimensional approach that is capable of capturing the downstream propagation of a floodwave and the response of flow to free surface slope, which can be described in terms of continuity and momentum equations as:

$$\frac{\partial Q}{\partial x} + \frac{\partial A}{\partial t} = q \qquad [1]$$

$$S_0 - \frac{n^2 P^{4/3} Q^2}{A^{10/3}} - \left[\frac{\partial h}{\partial x}\right] = 0 \qquad [2]$$

where Q is the volumetric flow rate in the channel, A the cross sectional area of the flow, q the flow into the channel from other sources (*i.e.* from the floodplain or possibly tributary channels), S_0 the down-slope of the bed, n the Manning's coefficient of friction, P the wetted

perimeter of the flow, and h the flow depth. Whilst suitable for fluvial flows, many coastal floodplains also contain channels that can have a significant influence on the development of inundation as they may provide routes along which storm surges may propagate inland or convey fluvial flood waters to the coastal floodplain thereby compounding flooding from coastal sources. The ability to represent channel flows was therefore retained in the version of the model designed for coastal flooding. For problems with no channels present this function can simply be switched off.

The term in brackets in Eq. 2 is the diffusion wave term, which forces the channel flow to respond to both the bed slope and the free surface slope. This can be switched on or off in the model to enable both kinematic and diffusion wave approximations to be tested. We assume the channel to be wide and shallow, so the wetted perimeter is approximated by the channel width. This approximation is suitable for typical natural channel geometries where the width-depth ratio is less than 10 (U.S. Army Corps of Engineers, 1993, appendix D). Eq's 1 and 2 are discretized using finite differences and a fully implicit scheme for the time dependence, and the resulting non-linear system is solved using the Newton-Raphson scheme. Sufficient boundary conditions are provided by an imposed flow at the upstream end of the channel section for the kinematic channel flow model, while for the diffusion wave model this must be supplemented by an imposed water elevation or water surface gradient at the downstream end. The channel is discretized as a single vector along its centreline separate from the overlying floodplain raster grid. The channel thus occupies no floodplain pixels, but instead represents an extra flow path between pixels lying over the channel. Floodplain pixels lying over the channel have two water depths associated with them: one for the channel and one for the floodplain itself. At each point along the vector the required channel parameters are the width, Manning's n value and bed elevation. The latter gives the bed slope and also the bankfull depth when the channel vector is combined with the

floodplain Digital Elevation Model (DEM). Each channel parameter can be specified at each point along the vector and the model linearly interpolates between these. This interpolated channel is then used to identify cells in the overlying floodplain grid which have a channel lying beneath them. The only constraint on this procedure relates to the bed elevation profile. As with other channel parameters, this can have a gradient which varies along the reach, and which may also become positive (i.e. trend upwards) if the diffusive wave model is used. However, use of the kinematic wave approximation requires that the down reach slope must be everywhere negative.

When bankfull depth is exceeded, water is transferred from the channel to the overlying floodplain grid. Floodplain flows are similarly described in terms of continuity and momentum equations, discretized over a grid of square cells, which allows the model to represent 2-D dynamic flow fields on the floodplain. We assume that the flow between two cells is simply a function of the free surface height difference between those cells (Estrela and Quintas, 1994):

$$\frac{dh^{i,j}}{dt} = \frac{Q_x^{i-1,j} - Q_x^{i,j} + Q_y^{i,j-1} - Q_y^{i,j}}{\Delta x \Delta y} \quad [3]$$

$$Q_x^{i,j} = \frac{h_{flow}^{5/3}}{n}\left(\frac{h^{i-1,j} - h^{i,j}}{\Delta x}\right)^{1/2} \Delta y \quad [4]$$

where $h^{i,j}$ is the water free surface height at the node (i,j), Δx and Δy are the cell dimensions, n is the effective grid scale Manning's friction coefficient for the floodplain, and Q_x and Q_y describe the volumetric flow rates between floodplain cells. Q_y is defined analogously to Eq. 4. The flow depth, h_{flow}, represents the depth through which water can flow between two cells, and is defined as the difference between the highest water free surface in the two cells and the highest bed elevation (this definition has been found to give sensible results for both wetting cells and for flows linking floodplain and channel cells). This is shown in Figure 1.

While this approach does not accurately represent diffusive wave propagation on the floodplain, due to the decoupling of the *x*- and *y*- components of the flow, it is computationally simple and has been shown to give very similar results to a more accurate finite difference discretization of the diffusion wave equation (Horritt and Bates, 2001a). The more complex treatment of floodplain flow yielded no significant improvement in the ability of the model to correctly simulate flood inundation when calibrated and compared against an observed inundation extent derived from satellite SAR data. However, the position of the performance maximum was shifted by the switch to a diffusion wave approximation for floodplain flows and the model became more sensitive to changes in floodplain friction.

Eq. 4 is also used to calculate flows between floodplain and any channels present in the domain, allowing floodplain cell depths to be updated using Eq. 3 in response to flow from the channel. These flows are also used as the source term in Eq. 1, effecting the linkage of channel and floodplain flows. Thus only mass transfer between channel and floodplain is represented in the model, and this is assumed to be dependent only on relative water surface elevations. While this neglects effects such as channel-floodplain momentum transfer and the effects of advection and secondary circulation on mass transfer, it provides a computationally simple solution to the coupling problem and should reproduce the dominant behaviour of the real system.

Previous sensitivity analysis and benchmarking studies with this code for fluvial applications have yielded detailed information on the behaviour of the code that should also hold true for coastal flooding applications given the similarity in physical processes. Comparison of LISFLOOD-FP to simple GIS procedures for estimating flood extent (Bates and De Roo, 2000), one dimensional St. Venant models such as HEC-RAS (Horritt and Bates, 2002) and full two-dimensional depth-averaged codes such as TELEMAC-2D (Bates and De Roo, 2000;

Horritt and Bates, 2001a; Horritt and Bates, 2002) have shown that when calibrated appropriately the model can simulate maximum inundation extent as well or better than alternative methods. Sensitivity studies (Aronica *et al.*, 2002; Bates *et al.*, 2004) have shown the model, like all other storage cell codes (e.g. that of Romanowicz and Beven, 1998), to be more sensitive to channel rather than floodplain friction. When the model is run within a Monte Carlo uncertainty analysis a wide range of friction parameter sets are typically found to fit available inundation extent data equally well. The model is therefore relatively robust to changes in the values used for floodplain friction.

Development of the LISFLOOD-FP model for coastal flooding applications was relatively straightforward. Boundary conditions for fluvial flooding applications normally consist of the time-dependent discharge in the compound channel at the upstream end of the reach, supplemented by the time varying water elevation or gradient at the downstream end of the channel when the diffusion wave representation of channel flow is used. Non-channel flow at the boundary of the domain is usually negligible and was not therefore included in the model. However, this is unlikely to be the case for coastal flooding applications. In addition, for fluvial applications the edge of the flow domain within the rectangular grid is normally defined topographically by steep valley side slopes at the edge of the floodplain. These are included in the Digital Elevation Model (DEM) that is the primary data source for the scheme. For coastal flooding, however, there is also a need to represent an irregular coastline within the domain as we do not wish to simulate flow in offshore areas. There are two reasons for this: first, offshore areas may comprise a large area of the model domain for which we do not require a risk evaluation, and second the simplified hydrodynamics in the LISFLOOD-FP code may break down in deep water. Consequently, the boundary condition representation was extended to allow specification of a time dependent discharge or stage either at the boundary of the rectangular grid or at points within the model domain. This can

be specified either as a time-varying mass flux or as a time-varying water surface elevation. In order to represent overtopping or breach discharge correctly, a standard weir equation (British Standards Institute, 1981) was included in the model and if the breach development is known this is also relatively easy to include by varying the DEM topography with time. The model does not, as yet, calculate the breach initiation and development directly based on geotechnical and hydraulic conditions and, in addition, requires discharge or water level to be specified at the overtopped structure. Lastly to allow the representation of an irregular coastline the ability to 'mask' areas of the DEM was introduced. This simply replaces the ground elevation value in a particular cell with an identifier which tells the model to not perform flow calculations or route water into that cell. This enables large offshore areas to be removed from the calculation procedure to represent the shoreline accurately and also serves to improve the computational efficiency for coastal applications.

3. Model evaluation

Hydrodynamic models are used to simulate a variety of flooding problems at a range of scales. A comprehensive testing procedure should therefore seek to evaluate model performance in as many of these situations as possible given sufficient data availability. The key data for the application of the LISFLOOD-FP model are: (1) an accurate DEM at a resolution appropriate to the modelling problem at hand and information on defence crest elevations; (2) boundary condition data, such as defence overtopping discharge by waves or water surface elevations to represent defence overflow, through the full dynamic event; (3) friction parameters which are usually unknown *a priori* and found through a calibration procedure and (4) a source of validation data. Characteristically, field applications of two-dimensional hydrodynamic models are usually calibrated and validated against point data on water surface elevations, flow velocity and direction acquired from boat campaigns at a small number of locations (see for example Kashefipour *et al.*, 2002; Sutherland *et al.*, 2004) and if

sufficient data exist then split sample testing is undertaken. Whilst such data can be highly accurate, they do not test distributed model performance across the whole domain. For risk-based shoreline management, we require models capable of yielding maps of flood inundation extent that are accurate *everywhere*, and this cannot be directly and explicitly tested using point measurements. Thus, if we wish to develop and comprehensively test models for coastal flooding we need to compare models to observations of the quantity of interest, in this case flood inundation extent.

Consistent, wide area data on inundation extent are relatively uncommon given that recording of such information is not a priority for civil defence agencies during a major coastal disaster. Moreover, the need for accurate data on topography and flow boundary conditions for large, hazardous events constrains availability further still. However, sufficient data sets for a variety of coastal flooding problems do exist to allow an initial assessment to be made of the ability of LISFLOOD-FP to simulate coastal flooding. Three locations, all from the UK (see Figure 2), were identified where data sufficient to parameterize and validate the LISFLOOD-FP code could be obtained. These represented two examples of local scale flooding caused by defence breaching and wave overtopping and a regional scale breach event. In addition, a fourth test case was added which represents the inundation of low-lying areas along a major densely-populated estuary given a range of sea-level rise scenarios. No validation data existed for the latter test case but it has been included here to demonstrate the ability of the LISFLOOD-FP model to rapidly compute a large number of scenarios to aid future planning. The uncertainty associated with each data set may necessarily be large given the difficulty of obtaining critical measurements (such as of defence overtopping rates) whilst an event is in progress. In north-west Europe coastal flooding is usually a winter occurrence, and short daylight periods mean there is a much higher probability that coastal flooding will happen at night which may make data collection even more hazardous, if not impossible. Much of what

we know of particular floods is therefore derived through forensic post-event reconstructions conducted by management authorities to learn lessons from the disaster. The modelling case studies described in this paper are therefore based on these official reports as these represent the best available understanding of how and why the flooding developed. However, the uncertainty in these data is likely to be high, particularly compared to the equivalent data for fluvial flooding (see for example Bates and De Roo, 2000), and the conclusions drawn should be viewed accordingly.

In each case, the goodness of fit between observed and predicted inundation extent was quantified using the performance measure:

$$F = \frac{A_{obs} \cap A_{mod}}{A_{obs} \cup A_{mod}} \quad [5]$$

Where A_{obs} and A_{mod} represent the sets of pixels observed to be inundated and predicted as inundated respectively. F is equal to 1 when observed and predicted areas coincide exactly, and 0 when no overlap exists. F is well suited as a performance measure for coastal inundation models as it excludes areas observed dry and predicted dry by the model. This largely prevents any bias to the measure as a result of domain size, given that it is relatively easy to predict correctly a small flood in a large and predominately dry domain. F should therefore be relatively consistent when comparing applications with domains that differ in size and hence has been used for all the comparisons reported in this paper. Details of the four case studies are summarised in Table 1.

3.1. Overtopping and breach of local defences: Towyn, North Wales, UK

Towyn is a small town on the North coast of Wales in the UK built on large areas of coastal lowland reclaimed during the 18th century. Towyn was inundated in February 1990 when 467m of seawall was breached by a 1 in 500 year event which occurred when a 1.3m storm

surge coincided with a high tide and 4.5m high waves. A lack of natural protection meant that the seawall, which had been in need of maintenance, felt the full force of the waves. The extensive low gradient coastal floodplain topography resulted in the flood reaching as far as 2km inland with a maximum depth of 1.8m. Although there were no direct fatalities, 5000 people were evacuated from nearly 3000 properties and immersion of agricultural areas resulted in damage to crops. The total cost of the flood was estimated as being in excess of £50 million (HR Wallingford, 2003).

Towyn is situated on the estuary of the river Clwyd. A previous study (HR Wallingford, 1985) indicated that water levels in the estuary are controlled by astronomical tides alone. A more recent study (HR Wallingford, 2003) reports that the embankment crests in the estuary are unlikely to be exceeded by the storm surge water level and are ignored for the purposes of this case study. The remaining defence system comprises 14 coastal defences, of which only one was breached during the 1990 floods. These are currently all protected by a shingle beach that is recharged in places. The defences vary in type from sea walls to dunes with crest heights ranging from 7m to over 9m above mean sea level.

The Towyn flood was relatively well documented and this provides a means of validating hydrodynamic models. A recent study undertaken by HR Wallingford (2003) provided information on defence crest levels, wave and water level distributions, overtopping discharges and defence fragility. A DEM constructed from IFSAR (Interferometric Synthetic Aperture) data (Colemand and Mercer, 2002) was also available. This was provided as a 'bare earth' DEM with a horizontal resolution of 5m and a vertical accuracy in terms of the root mean square error (rmse) of ~1m. This was further supplemented in densely populated regions of the DEM with locally surveyed manhole data with a vertical accuracy of 0.05m rmse. These were used to compensate for errors in the vegetation removal algorithms used to

construct the 'bare earth' DEM by favouring the surveyed manhole data in the final DEM where they existed.

At Towyn, the LISFLOOD-FP model was applied to a domain 12.5km by 9km at 50m resolution, giving ~45k models cells in total. The recorded tidal curve for the 1990 event and associated wave overtopping rates as estimated by HR Wallingford (HR Wallingford, 2003) were assigned as boundary conditions at the defences. These wave overtopping rates are likely to be subject to considerable uncertainty which was calculated by HR Wallingford (2003) as being, in this case, ±20-30%. In contrast, the tidal curve is likely to be much more accurate than this and we estimate the maximum error here to be only ±10cm. The full dynamic event lasting 62 hours was run using a model time step of 1s, giving ~223k time steps in total. As is standard in hydraulic modelling, the model was calibrated by comparing the predicted flood outline obtained using a number of different floodplain friction values to the observed maximum inundation extent from 1990 using Eq. 5. The observed outline was assumed accurate to ±100m in plan. In this case a trial and error procedure was used to find optimum friction values based on knowledge of model sensitivity acquired through fluvial studies (see Bates and De Roo, 2000). This calibration procedure yielded an optimum value of floodplain friction, n, of 0.06 in the urban areas nearer the coastline and 0.03 in the arable or sparsely populated areas further inland. The simulation was executed on a 2.5GHz desktop pc and took approximately 60 minutes. The mass balance error over the simulation was <1% of the total volume of water in the domain, as was the case for all simulations reported in this paper. For Towyn the optimum calibrated simulation resulted in an F value of 0.78. This compares to values of 0.64 to 0.85 obtained for applications of LISFLOOD-FP to fluvial flooding problem with similar data (Bates and De Roo, 2000; Horritt and Bates, 2001a; Aronica *et al.*, 2002; Horritt and Bates, 2002). For comparison we also computed the inundation extent using a simple GIS method by assuming a planar water surface across the

coastal floodplain at the level of the observed maximum water elevation of 5.85m. Intersection of this surface with the DEM also gives a predicted flood outline; albeit one that is neither mass conservative nor which respects hydraulic connectivity. Comparison of this prediction to the observed inundation extent yielded an F value of 0.48. Predictions from each model are compared to the observed flood extent in Figure 3.

Although the predicted shoreline from the LISFLOOD-FP model generally correlates well with the observed outline, there are two significant areas of inconsistency. An area in the south-western region of the flood outline is not flooded in the model as the DEM is in this region is significantly (~1-2m) higher than the observed water surface elevation. No alternative topographic data were available to improve the DEM in this region. The second inconsistency was at the south-eastern section of the model. Here, the model shoreline propagated further inland than the observed inundation extent. In this case it is likely that surface features not captured by the DEM helped limit the observed inundation extent and implies that a key requirement for future hydraulic modelling of this site is a more accurate topographic data set. The planar water surface calculation overpredicts flood extent significantly thereby demonstrating the requirement for at least a simple hydraulic model in this case.

3.2. Overtopping and breach and breach of local defences: Fleetwood, UK

Fleetwood is another small coastal plain town in the North-West of the UK (see Figure 2) which was inundated on 11th November 1977 due to a combination of high water levels and storm conditions. The water level return period for this event has been estimated to be ~30 years (Wicks *et al*., 2003). Structural damage of the upper part of one section of the sea wall defences occurred due to overtopping, but the main part of the defences did not fail. However, extensive overtopping took place along the length of the open coast. This caused

extensive hinterland flooding which was surveyed at the time thereby giving a data set suitable for inundation model validation. This consisted of a single shoreline vector, likely to be accurate to ±50m in plan.

Based on an assessment of the defence profiles at the time, the time-dependent overtopping rates along the coastline were estimated and supplied by the local council (Wicks *et al.*, 2003). This included an increased overtopping rate over a 100m section of the frontage to account for the single breach of the upper defence. Again, these are likely to subject to considerable errors, perhaps of up to ±50%, and as we here do not have more accurate tidal curve data for this event the boundary condition specification is more uncertain than that for the Towyn test case. Finally, for this site a DEM derived from airborne laser altimetry (LiDAR) conducted in 2000 was also available. This had a horizontal resolution of 2m and, for a flat unvegetated surface, a vertical accuracy of ~0.15m rmse. These data were processed to generate a 'bare earth' DEM by removing vegetation and building features using a standard algorithm, although visual inspection of the final DEM revealed that some obvious vegetation features still remained. These can be clearly seen in Figure 4, which shows the 2m resolution LiDAR DEM.

LISFLOOD-FP was applied to this data set at 10m resolution by spatially averaging the height data in the 2m DEM. The domain was also cropped such that its western and northern edges lay along the top of the sea defences and encompassed the area of observed flooding. The observed time dependent boundary fluxes along each segment of the coast were then assigned as model boundary conditions. Lastly, ground surveyed elevations along particular topographic features not well represented in the DEM, such as roads, were manually edited into the DEM file. Given the complementary between the LISFLOOD-FP discretization and

common Geographical Information System (GIS) data formats, the total set up time was less than one person-day.

The model grid consisted of 230 x 630 cells, giving a total of ~145k cells. The entire 12.5 hour dynamic event was simulated on this grid using 18000 time steps each of 2.5s duration. Simulation times on a 2.5GHz processor were of the order of 5 minutes. Sensitivity tests showed that varying Manning's n made only a minor difference to the maximum predicted inundation extent in this case. Accordingly, a floodplain friction value of n = 0.06 was therefore assigned to the whole domain, which for this application yielded an F value of 0.54. Given that only wave overtopping rates and not water surface elevations were available it was not possible at this site to compare LISFLOOD-FP to a GIS calculation of inundation extent using the planar water surface method in this case. Predicted inundation extent is compared to the observed shoreline in Figure 5, and appears better than the F value suggests. The low F value in this case seems, in part, due to the vegetation artefacts in the LiDAR DEM leading the model to predict spurious dry areas within the inundated area. In effect, the DEM records the vegetation height at these points and not the bare earth leading to a spurious topographic high point that cannot be inundated by the model. Hence, given uncertainty over the exact position of the observed shoreline and overtopping rates, possible changes in terrain between the 1977 event and the LiDAR survey in 2000 and incomplete removal of buildings and vegetation from the DEM this is a satisfactory result. Re-processing of the original LiDAR data may likely result in improvements to this model, however major uncertainties will remain concerning the prescribed overtopping rates and shoreline position that will fundamentally limit the information that can be obtained from this test case.

3.3. Regional scale flood modelling: East Anglia, UK

East Anglia contains large areas of low-lying land which were reclaimed from the sea over many centuries. Much of this is below the level of mean high water spring tides and therefore highly susceptible to flooding. The majority of the coastline is defended by a system of dunes, groynes and seawalls. Flooding in East Anglia has occurred a number of times over the last 100 years, most notably in 1907, 1938 and 1953 (Mosby, 1938, Steers, 1953). The 1938 storm surge resulted in a breach in the Winterton dunes, nearly 500m in length. This led to the inundation of approximately 30km^2 of coastal hinterland for which the inundation extent, breach development and maximum water level at the breach were well documented by Mosby (1938). The 1953 storm surge did flood properties at Sea Palling and surged up the river Yare resulting in inundation at Great Yarmouth, however only limited information on the resulting flood outline is available.

A DEM for this region was constructed from LiDAR data which has a horizontal resolution of 2m and vertical accuracy of ~0.15m rmse. The LiDAR data were passed through a standard vegetation removal algorithm, although as at Fleetwood, visual inspection of the data revealed that in urban areas some features still remained. The model covered the coastline from Sea Palling to Lowestoft and extended inland as far as Norwich (see Figure 2). This region was discretized on a 250m cell grid consisting of 161 x 168 cells, giving a total of ~27k cells, covering an area of 1700km^2. Flow within the floodplain is heavily influenced by a complex series of embankments; some constructed around rivers and drainage channels to provide fluvial flood protection and others to support road or rail infrastructure. However, their presence often restricts the flow of water within the floodplain, particularly for lower return period flood events. Spatial averaging of the 2m resolution LiDAR data to the model grid scale results in these features being ‘smeared out’, so their influence was simulated by defining weirs at the appropriate crest elevation and location within the floodplain.

Both the 1938 and 1953 events were simulated with this model. For the 1938 event the DEM was modified at Winterton to include the breach dimensions given by Mosby (1938). Unfortunately, no dynamic time series of water levels over the 1938 event was available and the only boundary condition information consisted of the maximum recorded water level at Winterton. To allow a dynamic simulation we therefore took the time series of water levels for the 1953 event as recorded at Sheerness (see Figure 6) and re-scaled this to the maximum water level given by Mosby (1938). We assume that the shape of the 1953 event to be typical of storm surge waves along the eastern coast of the UK and believe, despite the uncertainty introduced by this procedure, this to be the best approximation available given the lack of data.

The entire 10 hour dynamic event was simulated using 36000 time steps of 1s duration. On a 2.5GHz processor, simulation time was 5 minutes. The model was more sensitive to Manning's n than at Fleetwood and Towyn. This is predominantly because the floodplain has a low gradient, and initially there is a negative gradient before the land starts to rise to high ground. As at other sites a number of values of Manning's n were tested and n=0.025 gave a very good model performance of F value of 0.91. Application of the planar water surface model in this case led to large areas of the coastal floodplain being predicted as flooded compared to the relatively limited extent of flooding suggested by the observed data. This process yielded an F value of only 0.11 and suggests that the planar method is even more susceptible to failure in wide area applications where there is a greater possibility of low points in the DEM being below the elevation of maximum flood level but not hydraulically connected to the flood. Predicted inundation extent is compared to the recorded inundation extent for both LISFLOOD-FP and the planar method in Figure 7.

For the 1953 surge event model boundary conditions consisted of the water elevation time series shown in Figure 6 without re-scaling of the maximum elevation. At Great Yarmouth, the landward extent of inundation was not available. However, flood information within Yarmouth town centre was known and using n=0.025 the model correlates well with the areas known to have been inundated, providing further confidence in the calibration.

3.4. Inundation from extreme sea level rise scenarios: Thames estuary, UK

There is a great deal of uncertainty as to future changes in sea level (e.g., Hulme *et al*., 2002). The rate of sea level rise (SLR) is governed by many factors (in some cases opposing). Thermal expansion of sea water as a result of global warming and melting of land-based small glaciers and the Greenland ice sheet will all result in increased SLR, whereas the growth of the Antarctic ice sheet or increased terrestrial storage of water resources by humans could act to reduce SLR. However, it is believed that the collapse of the Western Antarctic Ice Sheet (WAIS) may result in a SLR of up to 5-6m (Mercer, 1978; Oppenheimer, 1998). This comprises an abrupt change in climate and hence, a low probability/high consequence part of the risk profile (Hulme, 2003). The likelihood and speed of WAIS collapse is highly uncertain: this model analysis was designed to support a study of the process of adaptation to abrupt climate change (in essence a sensitivity analysis) so the probability of the event is less important. Dawson *et al*. (in press) justify and discuss this modelling in more detail, however, a limited number of results are presented here to demonstrate how LISFLOOD-FP is suited to modelling this type of problem.

The tidal Thames is a drowned river valley with a morphology typical of coastal plain estuaries with extensive tidal mudflats (Dyer, 1973). Simulation of inundation over low-gradient tidal floodplains with significant flood defence structures (embankments, etc) requires at least a two-dimensional modelling approach with relatively high spatial resolution

(grid scales 250m or less) to represent the complex geometry. However, full two-dimensional modelling of the whole Thames estuary remains computationally prohibitive at this scale, particularly if one wishes to simulate multiple scenarios associated with different potential futures.

Given the need for estuary-scale two-dimensional modelling within a probabilistic framework, LISFLOOD-FP was applied to the tidal Thames. As we consider only large surge events, we can assume that gravitational forcing due to the tidal range at the estuary mouth is the dominant driving force and that the simplified flow representation in LISFLOOD-FP is adequate to capture this. By using LISFLOOD-FP we also assume implicitly that the inflow of saline water dominates and that the estuary is well mixed and of constant density. Unlike the previous three test cases, adequate validation data for this study site does not exist as the flood defences have successfully prevented recent flooding. The last major flooding of the Thames tidal floodplain occurred in response to the 1953 event, however no consistent inundation extent map considered sufficiently reliable for model validation exists despite (or perhaps because of) the scale of the event. We therefore include this case merely as a further test of the strengths and weaknesses of the LISFLOOD-FP model and to demonstrate the utility of simplified two-dimensional models for scenario modelling and future planning for large scale strategic problems. In particular, this study demonstrates that LISFLOOD-FP can successfully handle large volumes of water in a large study domain.

The model was applied at 250m resolution using topographic data derived from airborne IFSAR (Interferometric Synthetic Aperture Radar) data (Colemand and Mercer, 2002). This data source for this site yields a DEM of 5m spatial resolution and vertical accuracy of 0.5m rmse that was coarsened to the model resolution by spatial averaging. This averaging should

act to improve the vertical height accuracy and the model scale DEM was further supplemented by known defence crest levels. Overflow of these defences was represented in the model using a standard weir equation (British Standards Institute, 1981). The model therefore consisted of a domain 140km by 60km starting upstream of the tidal limit (Teddington, near Kingston-upon-Thames) and extending east of Southend-on-Sea (see Figure 2). This covers an area of 8400km^2 represented with ~134k cells. The model was uncalibrated, as inundation records were unavailable, however, floodplain friction, n, was set at 0.1. This falls within the wide range of values used in other urban flood studies (*eg*. De Roo, 1999; Enel Hydro, 2001; Van Der Sande *et al*., 2003; Alkema, 2003), however model results are likely to be, to some extent, sensitive to the value selected and the choice of friction coefficient should be regarded as a modelling assumption.

Model boundary conditions were derived from statistical analysis of water levels in the estuary, shown in Table 2 and a typical storm surge history as shown in Figure 6. As flood risk in estuaries is dominated by defence overflowand defence breaching (Hall *et al*., 2003) we did not represent flow of water in the main channel. Rather boundary conditions were given as time series of water surface elevation imposed along the defence crests. This means that we do not require detailed bathymetric information in the estuary main channel, thereby considerably simplifying the modelling problem. Defence breach scenarios were not considered in this example which focussed upon the effects of extreme sea level rise that is so severe that all defences would in any case be overtopped. The present good condition of the Thames Barrier and flood defences downstream of it also means that failure is unlikely. The extreme nature of the events being modelled also means that the flood outline is relatively insensitive to defence breaches. The model simulated a range of flood scenarios, including the 1:1000 year flood for a number of extreme sea level rise scenarios in the estuary (between 1m and 5m net rise relative to the defences). The full 10 hour dynamic event shown in

Figure 6 was simulated in the model using 360000 time steps of 0.1s. On a 2.5GHz pc each simulation took approximately 6 hours to complete.

Key results from the hydrodynamic model are presented in Figure 8. These show the flood outline for the 1 in 1000 year flood event, given current defences for net sea level rise (SLR) scenarios of 1m, 3m and 5m respectively. The LISFLOOD-FP model produces results that are consistent with each other and intuitively correct, but at a computational cost that allows multiple scenarios to be evaluated. With the recent advent of cheap multi-processor computing, such a model could be run within a Monte Carlo framework with relative ease (see for example Beven *et al.*, 2000). The model results show that the topography of the Thames estuary floodplain is such that the area at risk from flooding increases most rapidly for the first 1m of SLR. Each additional 1m of SLR produces a smaller increase in the inundated area. In the worst case scenario of 5m net SLR approximately 1000km^2 of land and 1 million properties would be at risk from flooding from the 1000 year event (Figure 5). The approximate area inundated for the 1m and 3m SLR scenarios is 650 and 850km^2 respectively.

4. Conclusions

This paper has outlined a simplified two-dimensional hydrodynamic model, LISFLOOD-FP, for simulation of coastal floodplain inundation. The ability of this code has been assessed by comparison of model predictions with available observations of maximum inundation extent for three test cases representing a variety of typical coastal flooding situations at different scales. A demonstration of the ability of the code to simulate the flooding of tidal floodplains in a large estuary has also been presented. In each case for which data existed the model was, when calibrated appropriately, able to replicate the observed maximum inundation extent for the particular events to within the error of the observed topography, boundary condition and

model validation data. It is also clear from the sensitivity of model results to floodplain friction and the lower level of success of a simple GIS method for predicting flood extent in the two test cases where this could be applied that predicting coastal inundation requires at least a simple hydraulic model that respects the key hydraulic principles of mass conservation and flow connectivity. Moreover, the test cases clearly demonstrated the computational efficiency of the code and the ease with which applications can be constructed from DEMs given the synergy between the model discretization and typical data formats in Geographical Information Systems. The low computational cost confers an ability to evaluate thousands of model realisations, and potentially the model is capable of providing a principal component of a probabilistic framework for assessment of coastal flood risk.

It is clear that further research in this area will be fundamentally limited by the quality of the available data. Whilst the data sets presented in this paper are the best available for real world application of coastal flood inundation modelling yet encountered by the authors, they still contain considerable uncertainty, particularly for hydraulic boundary conditions, breach development and maximum flood extent. Data are rather better for fluvial flooding as such events are more frequent and here more meaningful benchmarking and sensitivity analysis of inundation models has been possible (see Horritt and Bates, 2002; Aronica *et al.*, 2002). Whilst we have here shown the ability of a specific simple model to replicate the available coastal flooding data to within limits imposed by its likely error, it is also probably that other models may be able to fit this data equally well. In this situation benchmarking studies are likely to add little to our existing knowledge of relative model performance, although the fact that available data can be replicated with simple models may perhaps imply that more complex methods may be over-specified given data and calibration uncertainties. A key requirement for research in this area is therefore the development of wide-area model validation data sets that will discriminate between competing codes.

Acknowledgements

Research presented in this paper has been funded through a number of projects and institutions. The Towyn study was undertaken as part of the "RASP: Risk assessment for flood and coastal defence systems for strategic planning" and was funded by the Environment Agency of England and Wales. Halcrow Group Ltd. funded the Fleetwood study. The East Anglia study was undertaken as part of the Tyndall Centre for Climate Change Research project (T2.6) "Regional assessment of coastal flood risk". The Thames estuary study was undertaken as part of the "Atlantis. North Atlantic Sea-Level Rise: Adaptation to Imaginable Worst Case Climate Change" project, funded by the European Commission FP5 (contract no. EVK2-CT-2002-00138). Data used in the case studies were provided by The Environment Agency, HR Wallingford and Wyre District Council.

References

Alkema, D. 2003, Flood risk assessment for EIA; an example of a motorway near Trento, Italy, in *Studi Trentini di Scienze Naturali: Acta Geologica*, **78**, 147-153.

Aronica, G., Bates, P.D. and Horritt, M.S., 2002. Assessing the uncertainty in distributed model predictions using observed binary pattern information within GLUE. *Hydrological Processes*, **16**, 2001-2016.

Aronica, G., Hankin, B.G. and Beven, K., 1998. Uncertainty and equifinality in calibrating distributed roughness coefficients in a flood propagation model with limited data. *Advances in Water Resources*, **22**, 349-365.

Bates, P.D. and De Roo, A.P.J. 2000. A simple raster-based model for floodplain inundation. *Journal of Hydrology*, **236**, 54-77.

Bates, P.D., Horritt, M.S., Aronica, G. and Beven, K. (2004). Bayesian updating of flood inundation likelihoods conditioned on inundation extent data. *Hydrological Processes*, **18**, 3347-3370

Battjes, J.A. and Gerritsen, H. 2002. Coastal modelling for flood defence. *Philosophical Transactions of the Royal Society of London Series A: Mathematical and Physical Sciences*, **360**, 1461-1475.

Bechteler, W., Hartmaan, S. and Otto, A.J. 1994. Coupling of 2D and 1D models and integration into Geographic Information Systems (GIS). In: White W.R. and Watts J. (eds.), *Proceedings of the 2nd International Conference on River Flood Hydraulics*, John Wiley and Sons, Chichester; UK, 155-165.

Beven, K J and Freer, J, 2001. Equifinality, data assimilation, and uncertainty estimation in mechanistic modelling of complex environmental systems. *Journal of Hydrology*, **249**, 11-29.

Beven, K J, Freer J, Hankin, B and Schulz, K, 2000. The use of generalised likelihood measures for uncertainty estimation in high order models of environmental systems. In W J Fitzgerald, R L Smith, A T Walden and P C Young (Eds), *Nonlinear and Nonstationary Signal Processing*,. Cambridge University Press, Cambridge, UK, 115-151.

Beven, K. 2002. Towards a coherent philosophy for modelling the environment. *Proceedings of the Royal Society of London Series A, Mathematical, Physical and Engineering Sciences*, **458 (2026)**, 2465-2484.

Beven, K. and Binley, A. 1992. The future of distributed models: model calibration and uncertainty prediction. *Hydrological Processes*, **6**, 279-298.

British Standards Institution. 1981. *BS3680: Methods of measurement of liquid flow in open channels, weirs and flumes*. BSI, London.

Colemand, M. D. and Mercer, J. B. 2002. NEXTMap Britain: Completing Phase 1 of Intermap's Global Mapping Strategy, *GeoInformatics*, December 2002, 16-19.

Dawson, R. J., Hall, J. W., Nicholls, R. J. and Bates, P. D. (in press). Quantified analysis of the probability of flooding in the Thames Estuary under imaginable worst case sea-level rise scenarios. *Int. J. Water Resources Development*, *Special Issue on Water and Disasters*.

Dawson, R. J., Hall, J. W., Sayers, P. B. and Bates, P. D. 2003. Flood risk assessment for shoreline management planning, in *Proceedings of the International Conference on Coastal Management*, Brighton, October 15-17, 2003, 83-97.

Dawson, R. J., Sayers, P. B., Hall, J. W., Hassan, M. A. A. M. and Bates, P. D. 2005. Efficient broad scale coastal flood risk assessment, in *Coastal Engineering 2004: Proceedings of the 29th International Conference*, Lisbon, Portugal 19-24th September 2004, edited by J. McKee Smith. New Jersey: World Scientific, 2005.

De Roo, A.P.J., 1999. LISFLOOD: a rainfall-runoff model for large river basins to assess the influence of land use changes on flood risk. In: *Balabanis, P. et al. (Eds.), Ribamod: River Basin Modelling, Management and Flood Mitigation. Concerted Action*, European Commission, EUR 18287 EN, pp. 349–357.

Dhondia, J.F. and Stelling, G.S. 2002. Application of one-dimensional-two-dimensional integrated hydraulic model for flood simulation and damage assessment. In Falconer, R.A., B. Lin, E.L. Harris and C.A.M.E. Wilson, (eds*)*, *Hydroinformatics 2002: Proceedings of the Fifth International Conference on Hydroinformatics. Volume One: Model development and data management*, IWA Publishing, London, 265-276.

Dyer, K.R. 1973. Estuaries: a physical introduction. John Wiley, Chichester, UK, 140pp.

Enel Hydro. 2001. *Development of rescue actions based on dam-break flood analysis, RESCDAM: Development of Rescue Actions Based on Dam-Break Flood Analysis*, Final Report: Appendix 12, European Commission.

Estrela T and Quintas L. 1994. Use of GIS in the modelling of flows on floodplains. In White HR and Watts J (eds), *Proceedings of the 2nd International conference on river flood hydraulics,* John Wiley and Sons, Chichester; UK, 177-189.

Gomes-Pereira LM and Wicherson R.J. 1999. Suitability of laser data for deriving geographical data: a case study in the context of management of fluvial zones. *Photogrammetry and Remote Sensing,* **54**: 105-114.

Hall, J.W., Dawson, R.J., Sayers, P.B., Rosu, C., Chatterton, J.B. and Deakin, R. 2003. A methodology for national-scale flood risk assessment, *Water and Maritime Engineering*, **156 (3),** 235-247.

Horritt, M.S. and Bates, P.D. 2001a. Predicting floodplain inundation: raster-based modelling versus the finite element approach. *Hydrological Processes*, **15**, 825-842.

Horritt, M.S. and Bates, P.D. 2001b. Effects of spatial resolution on a raster based model of flood flow. *Journal of Hydrology*, **253**, 239-249.

Horritt, M.S. and Bates, P.D. 2002. Evaluation of 1-D and 2-D numerical models for predicting river flood inundation. *Journal of Hydrology*, **268**, 87-99.

HR Wallingford. 1985. *Conwy estuary crossing field data collected by Hydraulics Research*, Report EX 1251.HR Wallingford, UK.

HR Wallingford. 2003. *Conwy Tidal Flood Risk Assessment, Stage 1 – Interim Report*, Report EX 4667, HR Wallingford, UK.

Hulme, M., Jenkins, G.J., Lu, X., Turnpenny, J.R., Mitchell, T.D., Jones, R.G., Lowe, J., Murphy, J.M., Hassell, D., Boorman, P., Mcdonald, R. and Hill, S. (2002), *Climate Change Scenarios for the United Kingdom: The UKCIP02 Scientific Repor*t, Tyndall Centre for Climate Change Research, University of East Anglia, Norwich, UK, 120pp.

Hulme, M. 2003. Abrupt climate change: can society cope? Philosophical Transactions of the Royal Society of London Series A: Mathematical and Physical Sciences, **361 (1810)**, 2001-2021.

Kashefipour, S.M., Lin, B., Harris, E. and Falconer, R.A. 2002. Hydro-environmental modelling for bathing water compliance of an estuarine basin. *Water Research*, **36 (7)**, 1854-1868.

Madsen, H. and Jakobsen, F. 2004. Cyclone induced storm surge and flood forecasting in the northern Bay of Bengal. *Coastal Engineering*, **51**, 277-296.

Meadowcroft, I.C., Reeve, D.E., Allsop, N.W.H., Diment, R.P. and Cross, J. 1996. Development of new risk assessment procedures for coastal structures. In Clifford, J.E. (Ed), *Advances in coastal structures and breakwaters*, Thomas Telford, London.

Mercer, J.H. 1978. West Antarctic Ice Sheet and CO2 Greenhouse Effect: A Threat of Disaster, *Nature*, **271**: 321-325.

Mosby J. E. G. 1938. The Horsey flood, 1938: An example of storm effect on a low coast, in *Geographical Journal*, **93 (5)**, 413-418.

Nicholls, R.J. 1995. Coastal Megacities and Climate Change. *Geojournal*, **37 (3)**, 369-379.

Nicholls, R.J. 2002. Rising sea levels: potential impacts and responses. In: Hester, R. and Harrison, R.M. (ed.) Global *Environmental Change: Issues in Environmental Science and Technology*, **17,** 83-107. (Cambridge, Royal Society of Chemistry).

Oppenheimer, M. (1998), Global warming and the stability of the West Antarctic Ice Sheet, *Nature*, **393**, 325-332.

Reeve, D. E. 1998. Coastal flood risk assessment. *Journal of Waterway, Port, Coastal and Ocean Engineering*, **124 (5)**, 219-228.

Romanowicz, R. and Beven, K.J., 1998. Dynamic real-time prediction of flood inundation probabilities. *Hydrological Sciences Journal*, **43**, 181-196.

Romanowicz, R. and Beven, K.J., 2003. Bayesian estimation of uncertainty for distributed hydrological models: estimation of flood inundation probabilities. *Water Resources Research*, **39 (3)**, art. no. 1073.

Romanowicz, R., Beven, K.J. and Tawn, J., 1996. Bayesian calibration of flood inundation models. In M.G. Anderson, D.E. Walling and P.D. Bates (eds), *Floodplain processes*, John Wiley and Sons, Chichester, 333-360.

Small, C. and Nicholls, R.J. 2003. A Global Analysis of Human Settlement in Coastal Zones. *Journal of Coastal Research*, **19 (3)**, 584-599.

Steers, J. A. 1953. The East Coast Floods, in *Geographical Journal*, **119 (3)**, 280-295.

Sutherland, J., Walstra, D.J.R., Chesher, T.J., van Rijn, L.C. and Southgate, H.N. 2004. Evaluation of coastal area modelling systems at an estuary mouth. *Coastal Engineering*, **51**, 119-142.

Turner, R. K., Subak, S. and Adger, W. N. 1996. Pressures, trends, and impacts in coastal zones: interactions between socio-economic and natural systems. *Environmental Management*, **20 (2)**, 159-173.

U.S. Army Corps of Engineers, 1993. *River Hydraulics Engineer Manual*. Report EM 1110-2-1416, Department of the Army, Washington D.C., USA, 176pp.

USACE 1996. *Risk-based analysis for flood damage reduction studies*, Report EM1110-2-1619, United States Army Corps of Engineers, Washington.

Van Der Sande, C. J., De Jong, S. M., and De Roo, A. P. J. 2003. A segmentation and classification approach of IKONOS-2 imagery for land cover mapping to assist flood risk and flood damage assessment, *Int. J. Applied Earth Observation and Geoinformation*, **4**, 217-229.

Venere, M. and Clausse, A. 2002. A computational environment for water flow along floodplains. *International Journal of Computational Fluid Dynamics***. 16 (4)**, 327-330.

Voortman, H. G. 2002. *Risk-based design of large-scale flood defence systems*, PhD Thesis, Delft University.

Vrijling, J.K. 1993. Development in probabilistic design of flood defences in the Netherlands, in *Reliability and Uncertainty Analyses in Hydraulic Design*, B.C. Yen and Y-K Tung (eds.) pp133-178, ASCE, New York.

Wicks, J., Mocke, R., Bates, P.D., Ramsbottom, D., Evans, E. and Green, C. 2003. Selection of appropriate models for flood modelling. *Proceedings of the 38th DEFRA Annual Flood and Coastal Management Conference,* 16th to 18th July 2003, Keele University, UK.

Figure captions

Figure 1: Representation of flow between cells in LISFLOOD-FP.

Figure 2: Map of the UK showing location of test cases.

Figure 3: Comparison of observed inundation extent for the 1990 Towyn flood with that predicted by the LISFLOOD-FP model and the planar water surface elevation method.

Figure 4: 2m resolution Digital Elevation Model (DEM) for the Fleetwood site derived from airborne laser altimetry (LiDAR). Note the presence of significant numbers of vegetation artefacts remain in the DEM even after processing to remove these.

Figure 5: Comparison of observed inundation extent for the 1977 Fleetwood flood with that predicted by the LISFLOOD-FP model.

Figure 6: The 1953 Thames storm surge as measured at Sheerness (Rossiter, 1954, Smith and Ward, 1998).

Figure 7: Comparison of observed inundation extent for the 1938 Horsey flood with that predicted by the LISFLOOD-FP model and the planar water surface elevation method.

Figure 8: The 1:1000 year flood outline for the Thames estuary after 1, 3 and 5m net SLR.

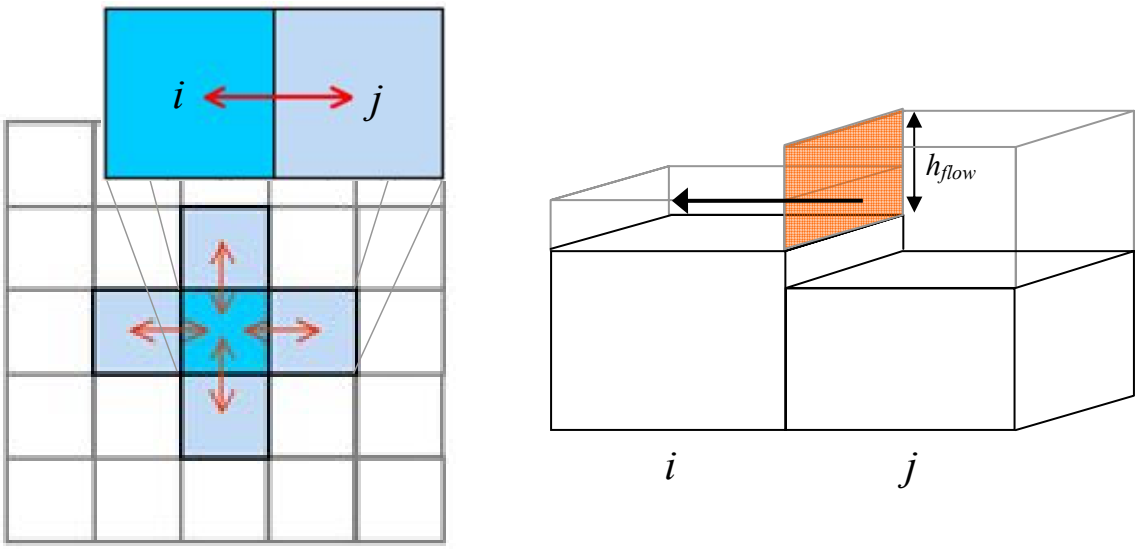

Figure 1: Representation of flow between cells in LISFLOOD-FP.

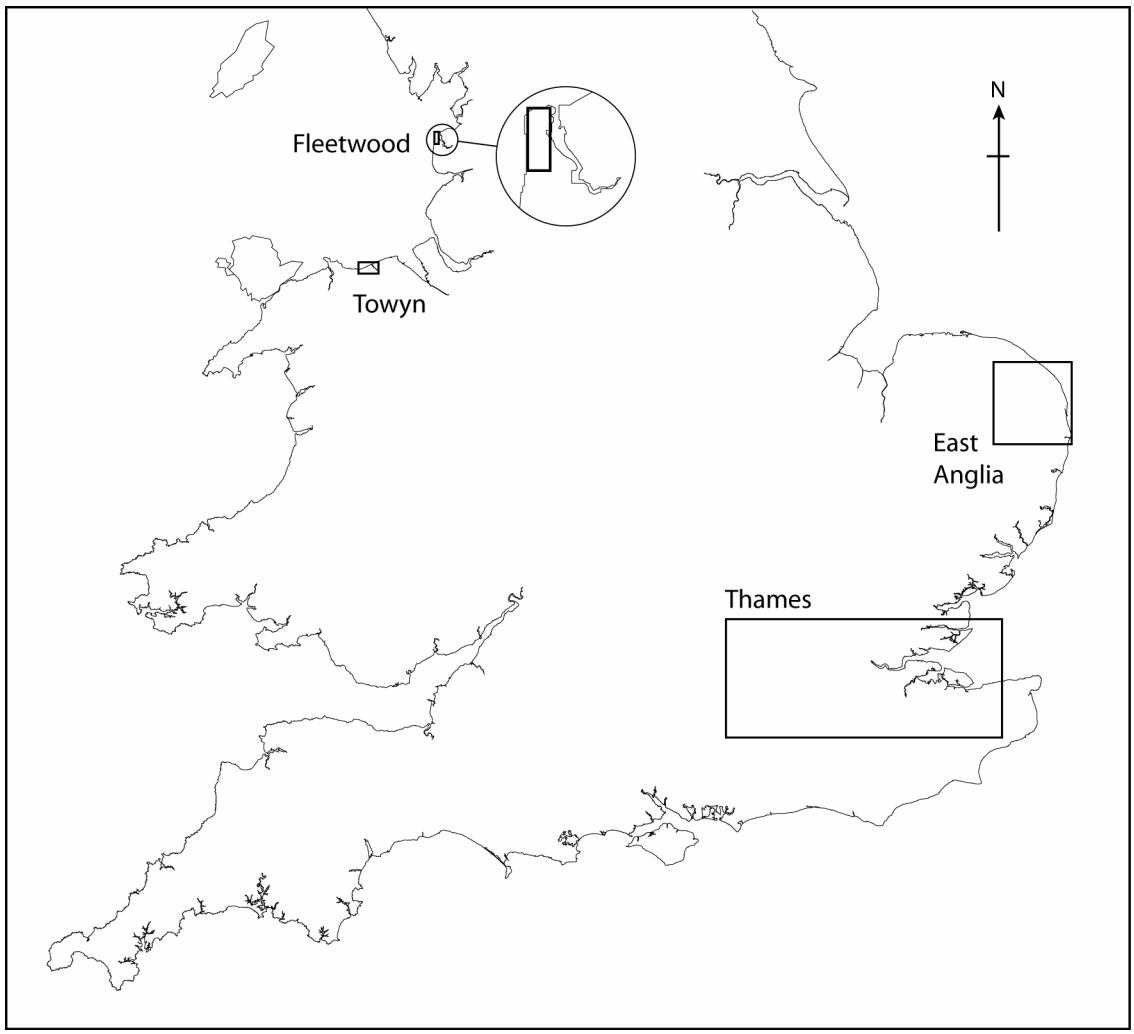

Figure 2: Map of the UK showing location of test cases.

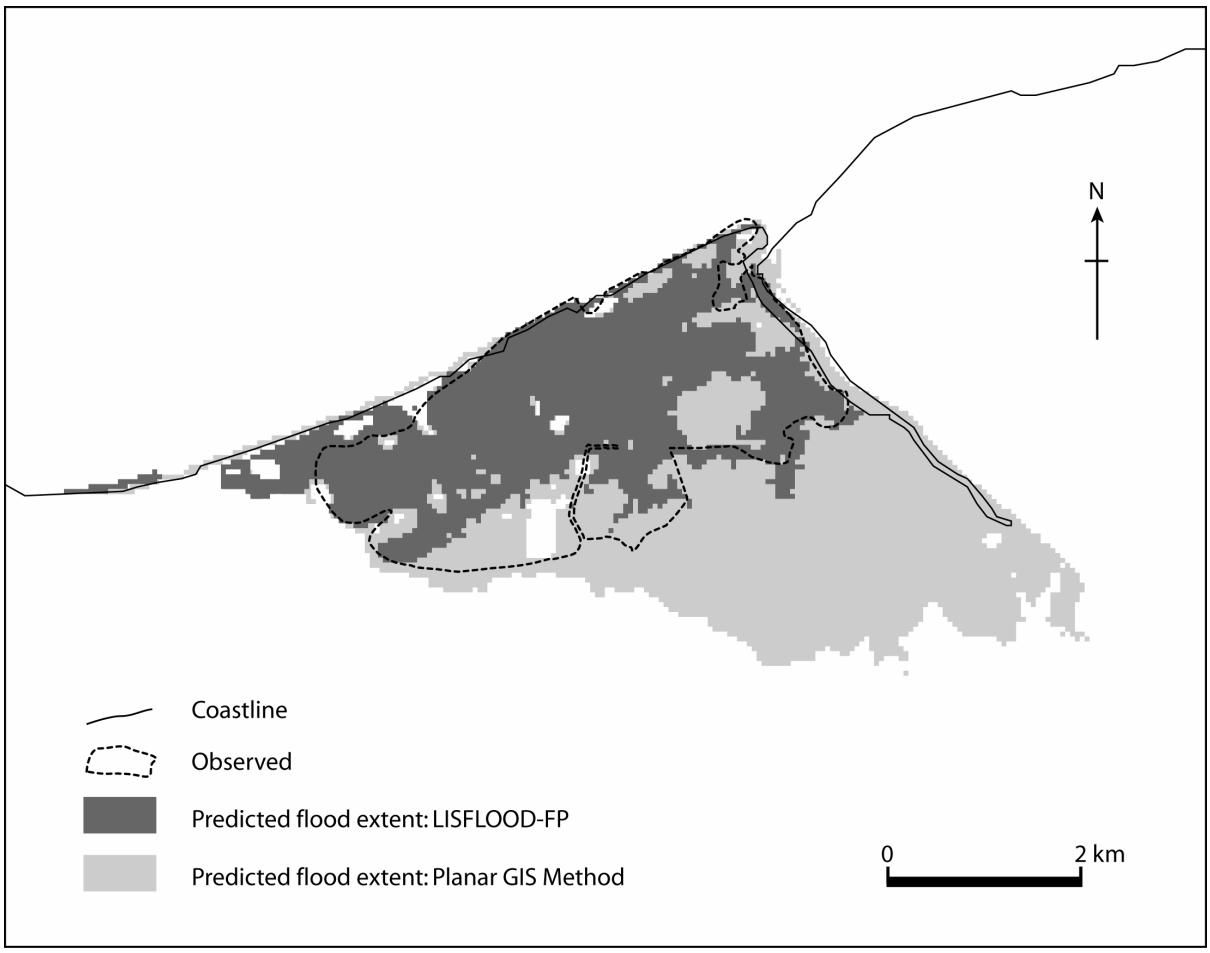

Figure 3: Comparison of observed inundation extent for the 1990 Towyn flood with that predicted by the LISFLOOD-FP model and the planar water surface elevation method.

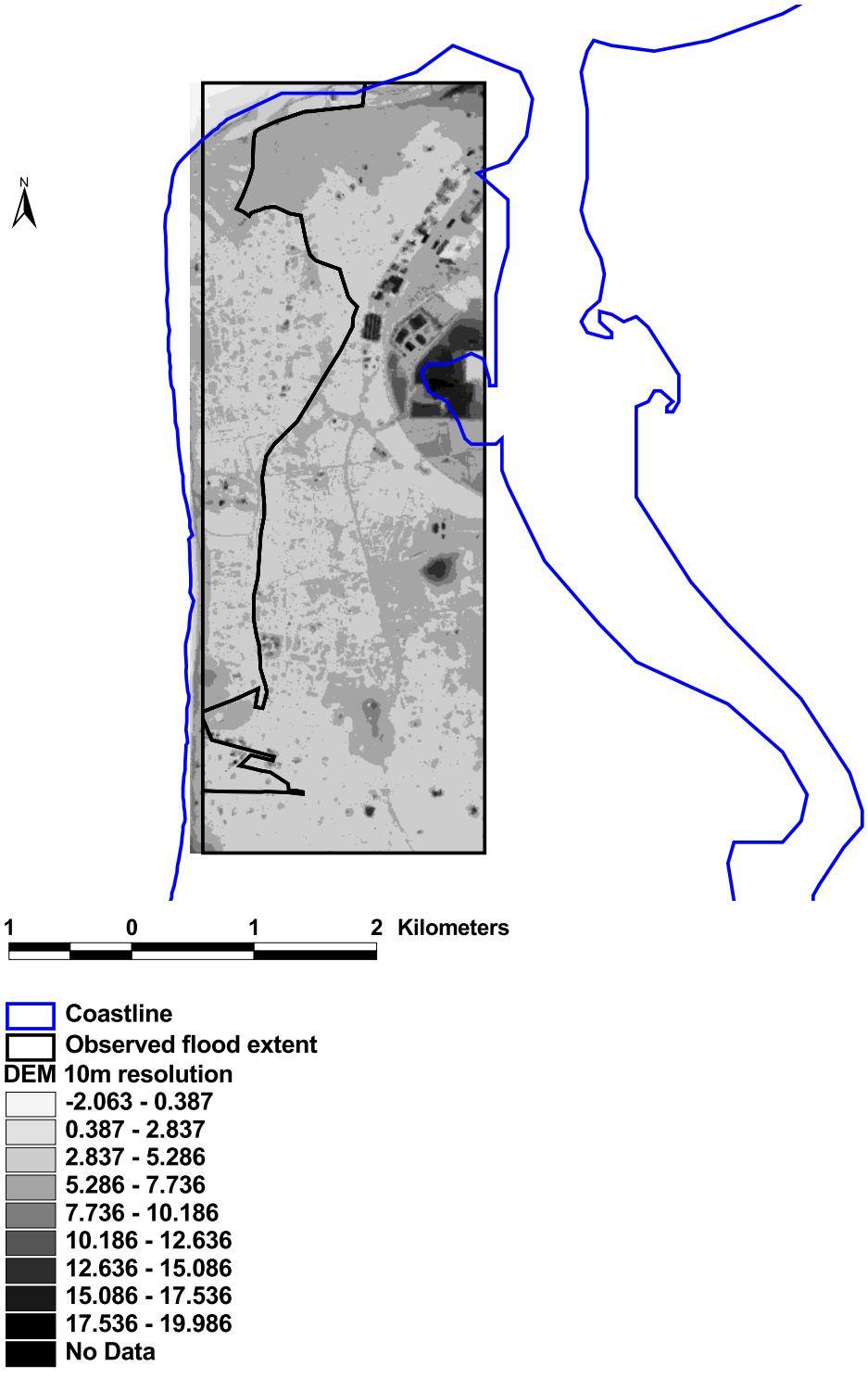

Figure 4: 2m resolution Digital Elevation Model (DEM) for the Fleetwood site derived from airborne laser altimetry (LiDAR). Note the presence of significant numbers of vegetation artefacts remain in the DEM even after processing to remove these.

Figure 5: Comparison of observed inundation extent for the 1977 Fleetwood flood with that predicted by the LISFLOOD-FP model.

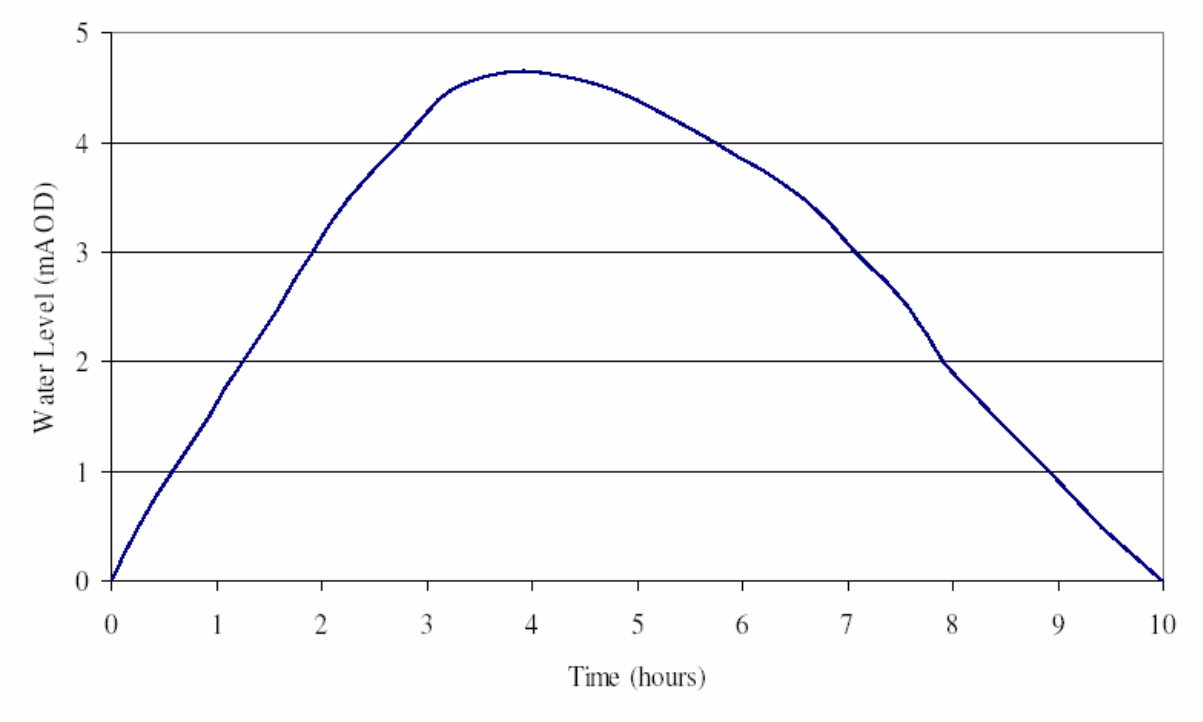

Figure 6: The 1953 Thames storm surge as measured at Sheerness (Rossiter, 1954, Smith and Ward, 1998)

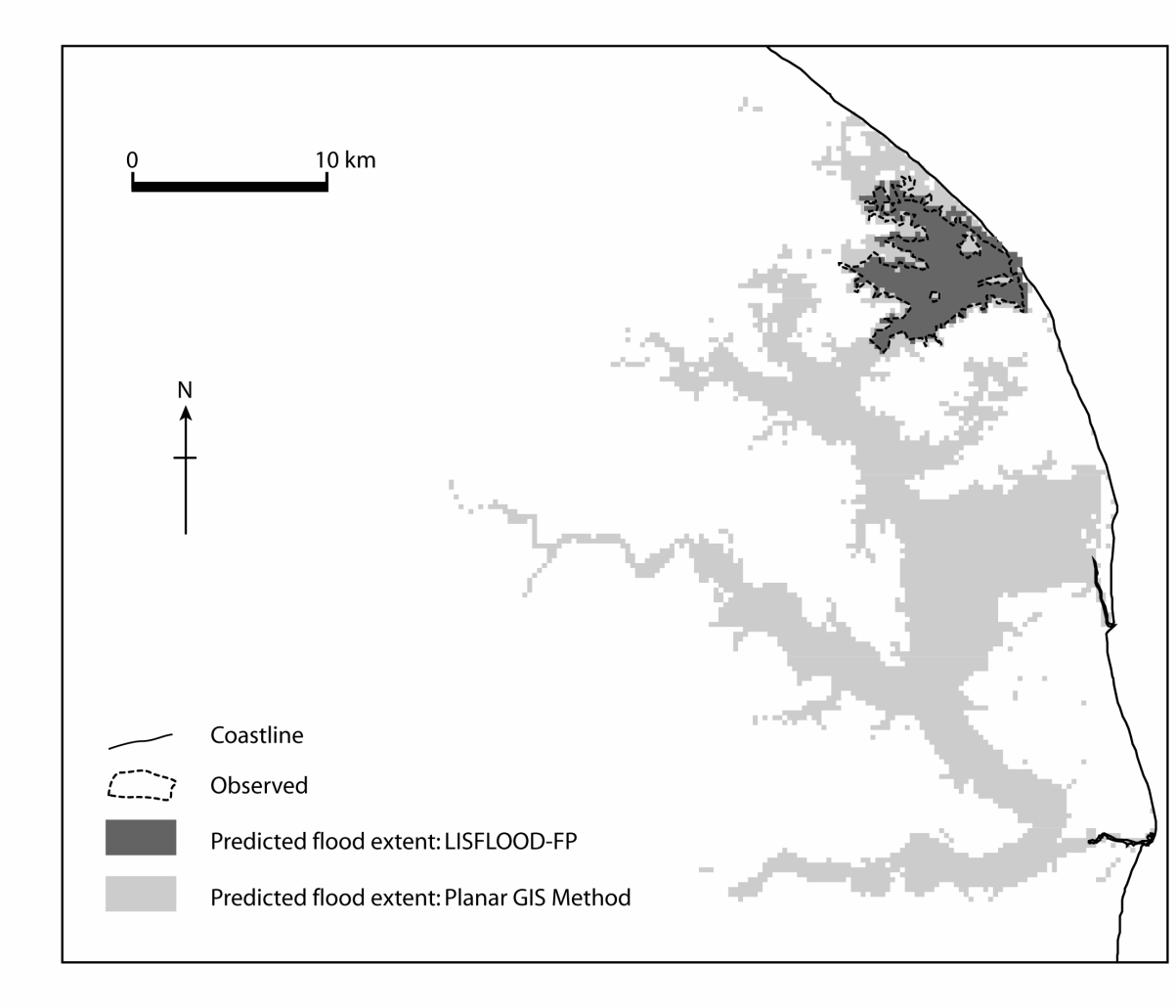

Figure 7: Comparison of observed inundation extent for the 1938 Horsey flood with that predicted by the LISFLOOD-FP model and the planar water surface elevation method.

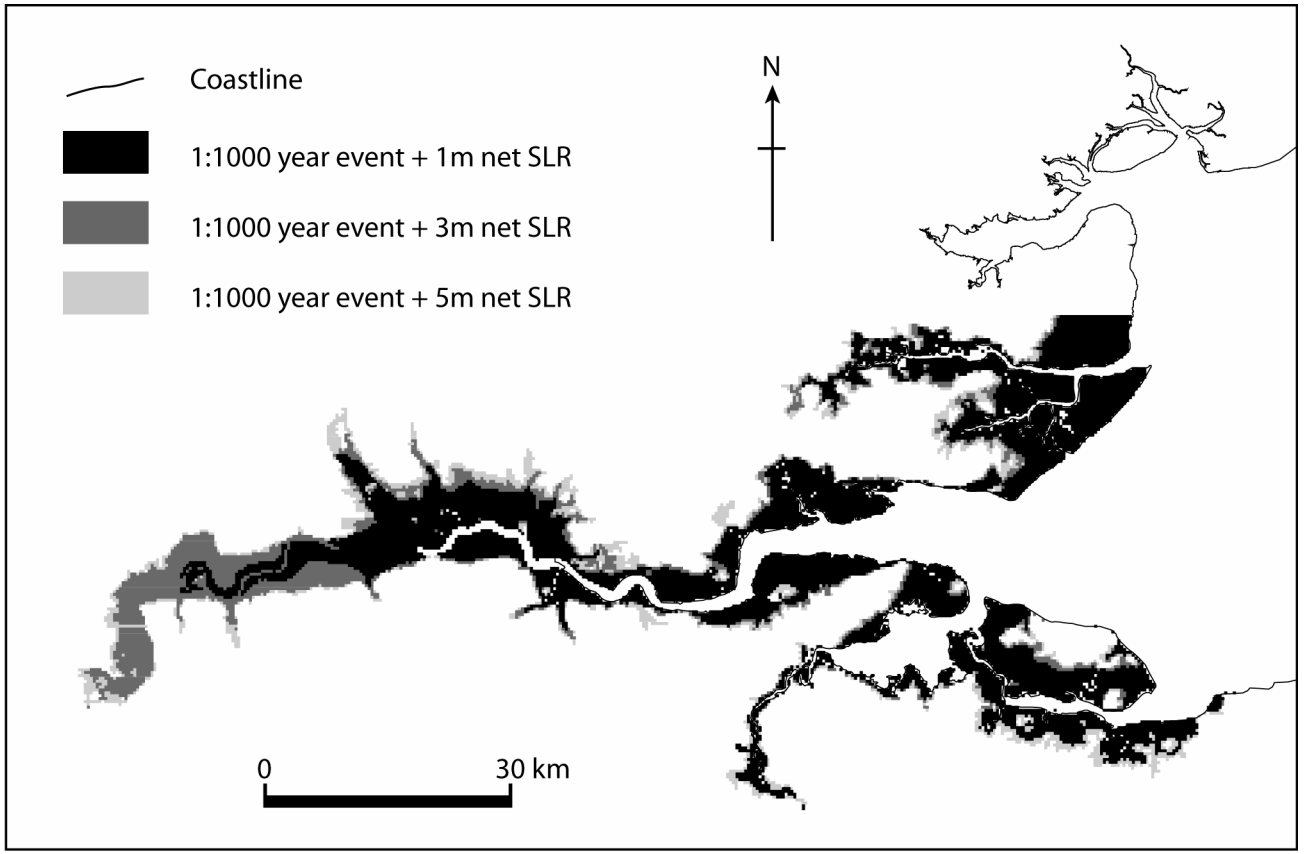

Figure 8: The 1:1000 year flood outline for the Thames estuary after 1, 3 and 5m net SLR.

Area	Type of flooding	Domain size	Grid resolution	Number of cells	Event	Model accuracy (*F*)	Computational time (on a 2.5 GHz pc)
Towyn, North Wales, UK	Defence overtopping	12.5 x 9 km	50m	~45k	62 hours of real time flow discretized as 223k time steps of 1s duration	0.78	~60 minutes
Fleetwood, UK	Defence overtopping	2.3 x 6.3 km	10m	~145k	12.5 hours of real time flow discretized as 18k time steps of 2.5s duration	0.54	~5 minutes
North Norfolk, UK	Defence breach	40.25 x 42 km	250m	~27k	10 hours of real time flow discretized as 36k time steps of 1.0s duration	0.91 for the 1938 event.	~5 minutes
Thames estuary, UK	Plain flooding and defence overtopping	140 x 60 km	250m	~134k	10 hours of real time flow discretized as 360k time steps of 0.1s duration	Not available	~6 hours

Table 1: Summary of the four test cases presented in this paper.

Site	**Return period**								
	2	5	10	20	50	100	200	500	1000
Silvertown (Thames Barrier)	5.21	5.44	5.61	5.77	5.95	6.11	6.29	6.51	6.70
Erith	5.10	5.33	5.50	5.66	5.87	6.02	6.21	6.43	6.62
Tilbury	4.66	4.89	5.03	5.19	5.37	5.53	5.70	5.91	6.09
Sheerness	3.89	4.08	4.20	4.33	4.49	4.62	4.77	4.96	5.12

Table 2: Return period of various water levels at sites within the Thames estuary.